George L. Bair
Gordon E. Carlson
University of Missouri
Rolla, Missouri 65401

Height Measurement with Stereoradar

Comparison of the effect of image dissimilarities on terrain height measurement for different stereoradar techniques.

Introduction

The generation of topographic data and topographic maps from radar images requires a pair of radar images of the desired terrain area. The two images must be obtained with different geometric characteristics so that differential image displacement (parallax) is present in the two images.[1,2] This parallax information can be measured and used to obtain terrain height data using analytic photogrammetric techniques.

The different elevation angles cause the two images of terrain points which are not on the reference plane to have different image displacements; therefore, terrain height information can be obtained. The resulting two images and radar shadows of a single vertical object are shown in Figure 2. The elevation angle difference (which must be large to provide sufficient image parallax) causes radar shadow differences and radar back-scatter (reflected radar energy) differences because the radar is supplying the scene illumination.

Abstract: *The effect of image dissimilarities on terrain height-measurement capabilities of three stereoradar techniques for obtaining stereoimage pairs is compared by using computer-generated simulated radar images. Simulated images are used because two of the stereoradar techniques are not presently implemented. The stereoradar techniques are: an improved single-flight technique, a previously proposed single-flight technique, and a two-flight technique which has been implemented. Improved stereoviewability is observed for the improved single-flight technique as compared with the pre-single-flight technique, and both single-flight techniques are better than the previously implemented two-flight technique. The improved stereoviewability of the single-flight images results in terrain height-measuring errors which are only 59 percent as large as those for the two-flight technique.*

The presently used technique that has been implemented for obtaining stereoradar image pairs utilizes a side-looking radar and two flights at different elevation angles with respect to the terrain being mapped. The flight geometry is shown in elevation view in Figure 1. As the radar is a range-measuring device, an elevated terrain point appears at the same position in the radar image as a terrain point on the reference plane which is closer to the aircraft position than the elevated terrain point orthographic position as is shown in Figure 1.

The requirement for two flights results in difficulty in establishing the relative aircraft position for the two images and thus produces difficulty in image registration. Together these effects degrade the stereoviewability and the topographic measurement capability. Also, it is a disadvantage to require two flights from a time-and-cost standpoint.

The generation of stereoimage pairs on a single flight with two radar antenna beams lying in vertical planes at different azimuth angles has been previously proposed. The

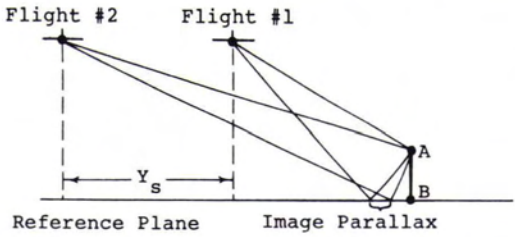

FIG. 1. Flight geometry for the two-flight technique.

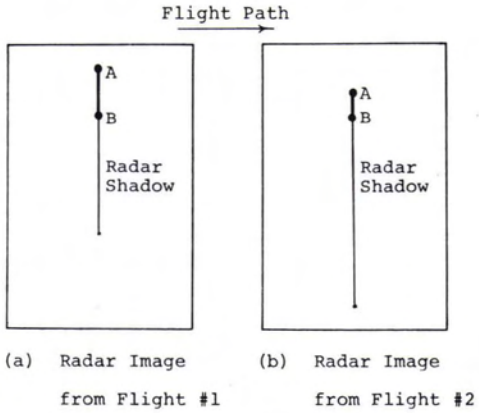

FIG. 2. Radar image pair for the two-flight technique.

concept is illustrated in plan view in Figure 3. The radar images obtained are similar to those previously shown except that the image displacement is in a different direction on each image. The two radar images have different image displacements because the aircraft position for illumination of the same terrain point for each image is different. The images are shown superimposed in Figure 4. This technique eliminates the two-flight requirement, but the difference in illumination angle (which must be large to provide sufficient image parallax) results in radar shadow differences and radar backscatter differences with their related image degradation.

The improved single-flight technique[3] uses one antenna beam lying in a vertical plane which is generated by a horizontal linear array mounted at an angle of $90\text{-}\theta_F$ degrees with respect to the flight path. This antenna beam is of the same form as that used for the forward beam of the previously proposed technique. The second radar antenna beam is a section of a cone with cone angle ϕ generated with a horizontal linear array parallel to the aircraft flight path by using appropriate phase weighting. The antenna beam geometry is shown in Figure 5 and the resulting two radar images are shown superimposed in Figure 6.

The angles θ_F and ϕ can be chosen so that terrain points being mapped are illuminated from very nearly the same aircraft position. This results in radar images that have nearly the same radar shadows and radar backscatter characteristics. Also, better image registration is possible because only a short distance is traveled by the aircraft between the two image recordings. As the conical antenna beam gives an image displacement which is perpendicular to the aircraft ground track, sufficient differential image displacement is available on the two images so that topographic data can be obtained.

A theoretical performance comparison of the three stereo techniques has been made.[4,5] The analysis was performed using system parameters chosen so that the three techniques are comparable. A desirable set of parameters for the improved single-flight technique was obtained by a complete tradeoff analysis. Parameters for the two previous techniques were then chosen to make the parallax obtained approximately the same for all three techniques with the constraint that the two-flight technique parameters be typical operational parameters. The theoretical performance parameters considered were

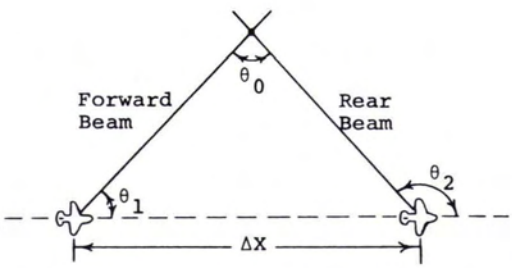

FIG. 3. Flight geometry for the previous single-flight technique.

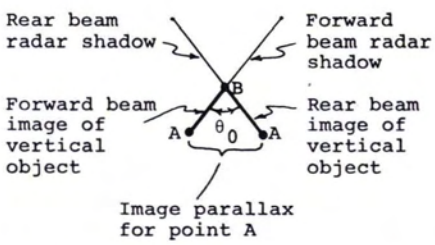

FIG. 4. Superimposed radar image pair for the previous single-flight technique.

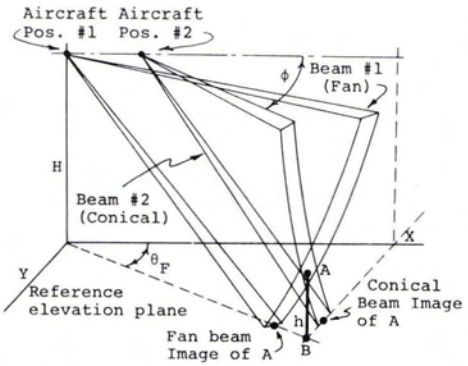

FIG. 5. Radar beam geometry for the improved single-flight technique.

those that affect the similarity of the two images in the stereopair obtained. The comparison of these parameters showed that the improved single-flight technique gives improved performance with respect to the previous single-flight technique, and both single-flight techniques give improved performance with respect to the two-flight technique.

The error performance for the three techniques has been analyzed.[4,5] The analysis was performed in terms of the sensitivities of the computed terrain point coordinates to system errors and in terms of the standard deviation of the error in the computed terrain point coordinates due to an assumed set of system error values. Comparison of the computed terrain point coordinate error due to system errors showed that the improved single-flight technique has the best error performance of the three techniques and that both single-flight techniques have error performance superior to the two-flight technique for an assumed reasonable set of error source values.

This paper discusses the use of simulated radar images for comparative evaluation of the effect of image dissimilarities for the three stereoradar techniques. Simulated radar images are used because there are no single-flight systems presently implemented; however, the simulated radar image characteristics approximate real radar images with sufficient accuracy to permit comparative evaluation of stereoviewability and image measurability.

Simulated Radar Image Generation

The radar image-simulation technique used for this analysis is capable of producing reasonably accurate simulated radar images with minimal complexity. A brief description of the technique is given in the following paragraphs. A more detailed description is available in Reference 6.

The terrain model of the region to be imaged is described in a two-dimensional coordinate system on a reference plane. The coordinates are defined with respect to the aircraft position as shown in Figure 7. The terrain is modeled by a set of equations which depend on the orthographic terrain coordinates x and y shown in Figure 7. The expression for terrain height is

$$h(x, y) = K \cdot P(x) \cdot Q(y)$$

where K is a terrain height scaling constant, and the functions $P(x)$ and $Q(y)$ are normalized terrain cross sections which are each piecewise functions of one orthographic coordinate. The mathematical terrain model obtained is an arbitrary shape where some attention to showing realistic features has been made. The terrain model used for this analysis is shown in Figure 8.

The simulated radar images corresponding to the selected terrain model were produced by a Calcomp Model 566 electromechanical plotter which was driven (off line) by plot commands generated by an IBM 360 Mod 50 computer. The software support available for the plotter allows positioning the pen and placing a variable size alphanumeric symbol

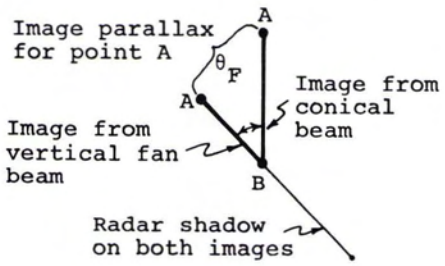

FIG. 6. Superimposed radar image pair for the improved single-flight technique.

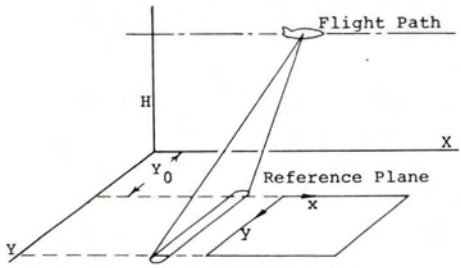

FIG. 7. Terrain reference coordinates.

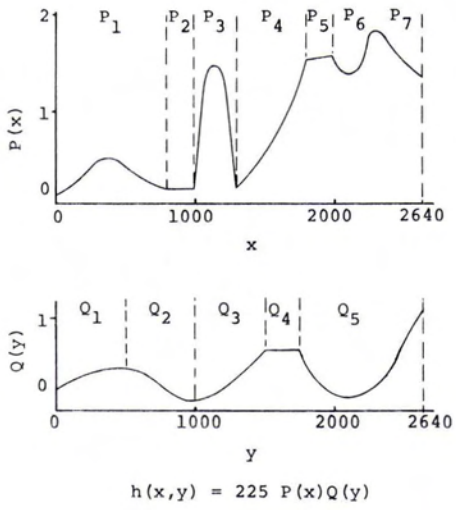

FIG. 8. Terrain model used.

in any desired location. If the symbol size is in the range of 0.020-0.050 inch it appears as a dot or blackened square. The method used to obtain the simulated radar image with the plotter is quite similar to the method used in printed matter to reproduce pictures by an array of equally spaced dots of varying size. If the dot spacing is small enough, the eyes cannot detect the individual dots, but instead see a composite shaded image. Each dot in the simulated radar image represents the radar return from a resolution cell size segment of the terrain.

The terrain characteristics, in a form compatible with the plotting technique discussed above, were obtained by initially dividing the terrain horizontal area into regularly spaced incremental areas corresponding to the size of a resolution cell. A small amount of random variation was then introduced in the incremental area spacing to break up the equal spacing of the incremental areas so that a realistic plotted image devoid of regularity could be obtained. The desired randomness was obtained by adding random increments to the x and y coordinates. These random increments had zero mean, were uniformly distributed, and had an absolute range of value of one-eighth the magnitude of the original point spacing.

If terrain is illuminated by a radar, the varying heights of the terrain cause displacements of the images of a terrain points from their true orthographic position as has been previously discussed. Also, the intensity of the radar return from various portions of the terrain is different because of the varying reflectivity for radar energy and change in terrain slope. To portray these effects, the dots used for each resolution cell in generating the simulated radar images have locations which depend on the characteristics of the radar system and the terrain height and have sizes which are a function of the intensity of the radar return.

A computer simulation was used to generate the image position and intensity values resulting from radar illumination of the terrain model with the various systems and also to convert these quantities into commands to drive the plotter. The data entered into the simulation program includes: size of the image to be produced, position of the image within the radar illumination swath, scale factors to be used, terrain point spacing, terrain model and technique geometry and parameters. The randomized coordinates of the centers of the terrain area segments were first calculated. The randomized orthographic coordinates for each terrain point were then used with the terrain model to determine the terrain height for each terrain point. The terrain point height and orthographic location were used together with the aircraft flight and radar parameters to obtain the image position for each terrain point on each image of the stereo pair.

The intensity, or brightness, of a given region of the simulated radar image depends on the fractional portion of the region covered by plotted symbols. For convenience, areas of maximum radar return were modeled as totally black and radar shadows were modeled as totally white. The plotted images were later photoreversed to produce images which have correct radar tonal relationships.

The density of the plotted symbols depends on their separation. For flat terrain this separation is fixed and was set equal (before randomization) to the resolution cell size. However, the separation decreases for terrain having a positive slope with respect to the aircraft position and increases for terrain having a negative slope. This change in separation is due to the varying image displacement which depends on terrain height.

The linear size of the dots was varied as the cosine of the incident angle of the radar illumination because this variation combined with the variation in dot spacing explained above results in a good approximation to the variation in radar return intensity which results from a rough surface for a radar antenna utilizing a radar beam pattern with cosecant-squared weighting in the elevation direction.[6] This type of radar beam pattern weighting is normally used for mapping radars to produce a more uniformly illumi-

nated image.[7] Therefore, in the computer simulation the incidence angle was computed and used to determine dot size.

Those portions of the terrain model that are shadowed, and thus give no return radar energy, must also be determined. This was done by determining individually whether each point was shadowed or illuminated. This was accomplished (using the terrain model height equations) by determining if any terrain was blocking the line of sight between the aircraft and the terrain point in question at time of illumination. No dot was plotted for shadowed terrain points.

Photo-processing of the plotter-generated simulated radar images must be done. The images as they appear from the plotter are the reverse of true radar images because areas of maximum return are displayed as totally black whereas shadowed areas are displayed as totally white. The simulated images were photoreversed so that correct tonal correspondence occurred for real radar images. Photoreduction of the plotted images was necessary so that they could be viewed at proper scales. Also, experimentation showed that slight defocussing of the images during photoprocessing enhanced the appearance of the simulated radar images as it diffused the dot pattern and thus provided a more realistic appearing simulated image.

Image Viewing and Measurement

Terrain points on vertical photographic images have displacements which are radial with respect to a point directly beneath the aircraft at the time the photograph is taken (image has central perspective). Image parallax for a resulting stereophotographic pair is in a direction parallel to the aircraft flight path. Thus photographic images are viewed with an eye base parallel to the aircraft flight path to obtain a stereoimage. In addition, if the viewer's eyes are located at positions which correspond to the scaled aircraft positions, then the entire image viewed has the correct proportions because it is formed from two central perspective images at their perspective points.

Terrain points on radar images have displacements which are all in the same direction. The resulting image parallax for a stereopair of radar images is approximately in a constant direction which depends on the particular stereo radar technique used. Therefore, a stereo view of the terrain can be obtained by viewing a stereoradar image pair if the correct image orientation is used. Correct proportions will not be preserved over the entire image because it is formed from

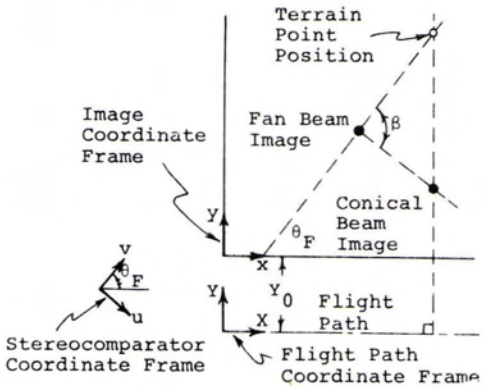

FIG. 9. Superimposed single-flight stereoradar images.

images which do not have central perspective. However, terrain height measurements can be made at points on the image using a stereocomparator to view and measure the image positions.

The image orientation required for a stereoimage pair obtained with the improved single-flight technique for viewing and measurement with a stereocomparator has been determined.[5] This orientation is also applicable to the previously proposed single-flight technique if forward and side-looking antenna beams are used because a side-looking beam gives the same image displacement as a conical beam. Figure 9 shows the superimposed image geometry for the single-flight techniques if the previously proposed single-flight technique is implemented with the forward and side-looking beams. The angle β is nearly 90 degrees for all practical terrain heights so measurements can be made by orienting the operator's eyes parallel to the u-axis. Images obtained with the two-flight technique are viewed with operator's eye base perpendicular to the flight path along the u-axis shown in Figure 10.

The simulated radar images which were viewed and measured for this analysis were obtained using the radar system parameters shown in Table 1. These parameters give systems having theoretical performance capabilities suitable for comparison purposes.[4,5] The simulated images were produced from the terrain model shown in Figure 8 which represents a 2640-ft square terrain area. The images produced were 4 inches square. This resulted in a plotting scale of approximately 1:8000. The images after photo-processing are shown in Figure 11 at a scale and placement suitable for view-

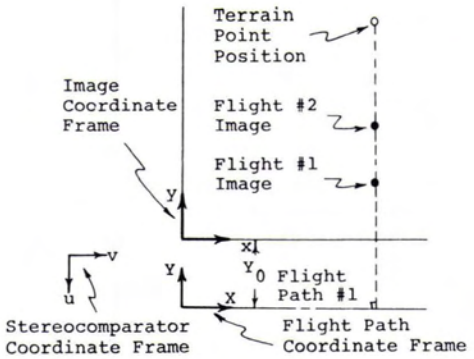

FIG. 10. Superimposed two-flight stereoradar images.

ing with a stereoscope. Note that the eyes should be parallel to the bottom of the page for viewing.

The plotted images were photo-processed so that they could be viewed with a steroecomparator to obtain terrain height measurement accuracy comparisons. The stereocomparator to obtain terrain height urement had a minimum image magnification of 13×. Thus, a 13× photo-reduction of the plotted images was required. Also photo-reversal was required so the images could be viewed with correct tonal relationships. Because of the large reduction required, defocussing was difficult to control and intentional defocussing was not used. However, there was some defocussing inherent with the photo-reduction and reversal. To be assured of the same photo-processing, all image pairs were placed on the same photographic plate.

For the performance evaluation that follows some method for identifying the terrain points being measured was necessary so that height measuring errors could be determined. This was accomplished by identifying and measuring relative maximum and minimum terrain heights only. This identification method was used because the identification of individual terrain points on the simulated radar images was a difficult and time consuming task for the stereocomparator operator. As the basic concern is evaluation of terrain height measuring capability, this identification method is entirely satisfactory.

Terrain Point Coordinate Computation

Equations which relate the terrain point image coordinates to the actual terrain point orthographic position and height coordinates are required to compute the terrain point coordinates from measured image position data. The form of these equations depends on the particular radar imaging geometry. The required equations for each of the three stereo radar techniques have been developed.[5] Several different sets of equations are possible for the single-flight techniques because there are four image position coordinates and three terrain point coordinates. The set that provides solutions which are least sensitive to system errors was chosen and is

$$x_R = x_2$$

$$y_R = y_1 + (x_2 - x_1) \tan \theta_F$$

$$h_R = H - \left[H^2 - y_{R^2 - Y_s^2}\right]^{1/2}$$

where x_1 and y_1 are the image position coordinates for the forward looking antenna beam, and x_2 and y_2 are the image position coordinates for the conical antenna beam or the side-looking antenna beam.

The solutions for the terrain point height, h_R, and the across flight path coordinate, y_R, are unique for the two flight technique because they depend only on the across-flight path image coordinates y_1 and y_2. The along-flight path terrain point coordinate, x_R, is obtained by averaging the two along-track image position coordinates. Thus the equations are

$$x_R = 0.5\,(x_1 + x_2)$$

$$y_R = (y_2^2 - y_1^2 + 2y_2Y_s) \,/\, 2Y_s$$

$$h_R = H - \left[H^2 + y_1^2 - y_R^2\right]^{1/2}$$

TABLE 1. SYSTEM PARAMETERS USED FOR PRODUCING IMAGES FOR COMPARISON TECHNIQUE.

Parameters	*Improved Single-Flight*	*Previous Single-Flight*	*Two-Flight*
Aircraft Altitude	15,000 ft.	15,000 ft.	30,000 ft.
Swath Width	2 mi.	2 mi.	2.5 mi.
Image Offset	12,000 ft.	12,000 ft.	29,000 ft.
Beam Geometry	75° Conical Beam Cone Angle 70° Fan Beam Angle	90° Side Beam Angle 70° Forward Beam Angle	90° Side Beam Angle

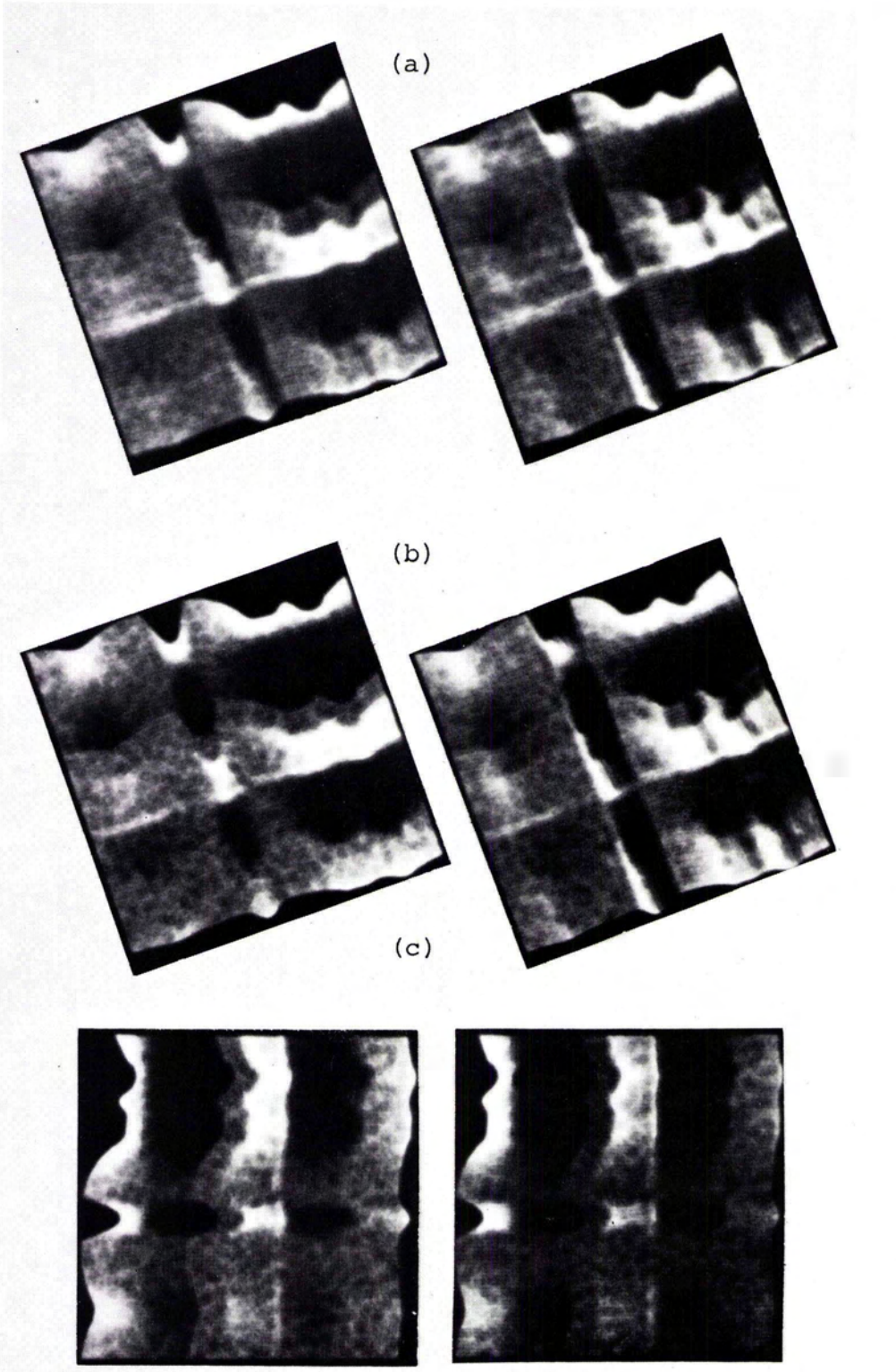

FIG. 11. Simulated stereoradar images pairs: *(a)* improved single-flight; *(b)* previous single-flight; *(c)* two-flight.

where x_1 and y_1 are the image position coordinates for Flight 1 and x_2 and y_2 are the image positon coordinates for Flight 2.

Estimation techniques similar to those used for photographic images must be applied to reduce system processing errors prior to the utilization of the above terrain point coordinate equations. The major error compensation techniques are discussed in the following paragraphs. The improved single-flight technique is used for discussing the techniques but they are applicable to all three stereoradar techniques.

First, a common image reference point must be determined for the two images of the stereo pair. The common reference point was determined from stereocomparator measurements of fiducial points placed on the images when they were produced. One image of a stereopair is shown in Figure 12 with fiducial points designated by coordinates u_{ij}, v_{ij}. Each fiducial point location was measured twice and the average measured value was used to determine the image center u_R, v_R by constructing the lines A and B and finding their intersection. The calculation was made for each image of the stereopair and the center points obtained were used as the common reference for the two images.

The improved single-flight radar images must be viewed at an angle (determined by the forward looking beam azimuth angle) with respect to the flight path. However, it is not possible to orient both images at exactly the same angle on the stereocomparator and thus the difference in viewing angle must be determined. This was done by using the fiducial measurements to calculate γ_1 and γ_2 as shown in Figure 12. The average of these angle measurements was then used as the average viewing angle for that image. The

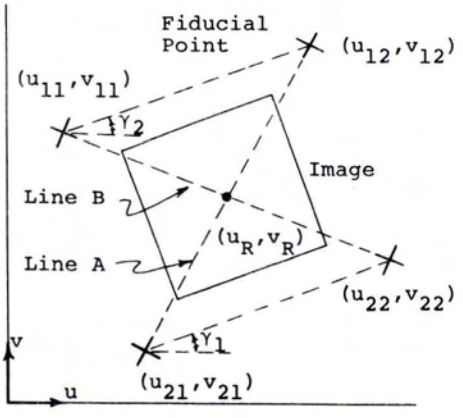

FIG. 12. Geometry of reference point and average viewing angle.

average viewing angle was calculated for both images and the difference between the two was taken as the rotational error. To correct this discrepancy, and in so doing gain rotational control, the conical beam image was used as a reference and the fan beam image was rotated about the center reference u_R, v_R to cancel the rotational error. This rotation results in a sample u, v-axis transformation for the forward-looking beam image.

All measurements obtained with the stereocomparator were in machine coordinates and had to be appropriately scaled and converted to the coordinate system of the terrain model. The scale factor used was determined by averaging the ratio of measured fiducial point separation to true scale separation for eight independent calculations between adjacent fiducial points on the two images. The coordinate conversion is a simple transformation from the u, v coordinate system using the reference angle previously determined.

The appropriate terrain point coordinate equations were used to calculate the orthographic location and height for each terrain point measured after the image control discussed above had been applied to the image measurements. The orthographic locations are the best obtainable; however, the terrain height values can be improved by using vertical control. To accomplish this, five of the terrain points were defined as control points. The measured control-point terrain heights were compared with the true terrain heights and the height errors were determined. Then, the original reference plane was replaced by a new reference plane which was determined so as to minimize the mean-square value of the height error in the control point measurements. The terrain point height for each terrain point measured was then computed with respect to this new reference plane.

Performance Evaluation and Comparisons

Stereopairs of simulated radar images for each stereoradar technique have been generated, processed, measured, and the measurement data used to obtain computed terrain point orthographic location and height. The height measurement errors obtained from the simulated radar images shown in Figure 11 for each stereoradar technique are shown in Table 2. The calculated sample means and standard deviations for the height measurements are:

Improved Single-Flight: $\mu_h = -0.30$ ft $\sigma_h = 5.7$ ft
Previous Single-Flight: $\mu_h = 0.90$ ft $\sigma_h = 5.7$ ft
Two-Flight: $\mu_h = 4.60$ ft $\sigma_h = 9.6$ ft

TABLE 2. HEIGHT MEASUREMENT ERRORS, Δh_R, FOR TERRAIN LOCAL MAXIMUM AND MINIMUM POINTS (Viewing Scale = 1:8000)

	Δh_R		
Terrain Point Height	*Improved Single Flight*	*Previous Single Flight*	*Two Flight*
14	1.7	4.0	−3.0
167	−6.4	−4.8	−6.9
17	−7.7	3.1	−4.7
188	7.2	6.0	−2.4
156	−10.0	−1.1	5.0
49	15.8	18.4	27.4
31	−0.3	6.2	18.3
38	4.0	7.2	14.5
34	5.5	5.9	9.9
3	1.0	−2.0	4.0
13	1.3	−0.9	−6.0
85	−2.0	−7.5	−0.7
19	−3.4	2.0	6.6
227	−0.6	−5.8	−11.8
24	−5.9	−4.2	11.7
256	5.9	−1.5	−2.1
213	1.4	−2.2	10.2
49	0.4	−2.6	200.5*
31	−4.0	3.1	226.1*
37	0.6	2.2	235.2*
3	−3.0	−4.7	10.3
33	−6.1	−2.0	8.6
3	−2.4	−0.1	3.9

All values in feet.

* These measurements are not included in calculating statistics.

The x, y statistics have not been given because exact horizontal identification was not used during the measurement.

The theoretical height measuring capability for the three stereoradar techniques has been computed with system parameters chosen to make the systems comparable. These computations were made with the assumption that image parallax on the radar images can be detected to the limit of one-half of the radar resolution. For equal resolutions, the three stereoradar techniques have approximately equal theoretical height measuring capability which gives a height measuring accuracy of approximately 45 ft for the system parameters used in generating the simulated radar images. The measurements are better than this theoretical limit due to the distinct dot patterns used on the simulated radar images measured that do not exist on true radar images. However, as the simulated radar images generated do contain the geometric and tonal aspects of actual radar return, they are useful in comparing the relative effect of image dissimilarity on the stereoviewability and terrain height-measuring capabilities of the three stereoradar techniques.

Comparison of the height-measuring capabilities determined from the simulated radar image measurements for the three stereomapping techniques shows that the improved single-flight and previous single-flight techniques give about the same performance and have height-measuring errors which are 59 percent of those obtained with the two flight technique. In addition, the stereocomparator operator making the measurements indicated that the improved single-flight images were easier to view and measure than the previous single-flight images and that both were easier to view and measure than the two-flight images. The reasons given for these differences in stereoviewability were the distinct shadow differences and differing intensity levels between images comprising the stereopair. These comparisons were made by the stereocomparator operator before he was told which should be best so that his results would be unbiased. Some regions on the two-flight images could not be viewed stereoscopically due to image differences. This is evidenced by the three terrain points with very large height measuring errors shown in Table 2. These points were not used in determining the error statistics.

For the stereomeasurements made, the degraded stereoviewability of the previously proposed single-flight technique with respect to the improved single-flight technique did not result in degraded terrain height-measuring performance. The performance should have been degraded an amount less than it is for the previously implemented two-flight technique. It is considered that the method of terrain-point identification used, and perhaps the characteristics of the particular single-terrain model used, may have obscured this smaller difference in height measuring capability.

SUMMARY

Simulated radar images were produced from a mathematical terrain model which resembles true terrain. The model was divided into segments whose sizes equal the resolution cell size of the radar system used. The segments were randomized to break up the regularity. For each segment on the terrain model, a small dot of varying size was plotted on each image comprising the stereopair.

The dot location was determined by the imaging geometry of the radar system used and the dot size was made proportional to the cosine of the angle of incidence of the radar energy upon the terrain. The resulting simulated radar images were photo-processed so that proper viewing scale and proper correspondence with actual radar imagery could be obtained.

Local maximum and minimum heights for terrain points were identified and measured for each stereoradar technique using standard photogrammetric equipment and techniques. The results were compared with the true terrain heights to determine the height-measuring capabilities of each of the stereoradar techniques. The results are better than the calculated theoretical limit due, in part, to the nature of the simulated image. However, the results can be used for comparison of image dissimilarity effects because the simulated images generated contain the geometric and tonal aspects of actual radar returns. The measurements show that the single-flight techniques have terrain height measuring errors which are 59 percent of those obtained with the two-flight technique. Also, the stereocomparator operator making the measurements indicated that the improved single-flight images were the easiest to view and measure, and that the previously proposed single-flight images were easier to view and measure than those for the two-flight technique. This was a result of greater image similarity.

ACKNOWLEDGEMENT

This work was supported by the Geography Programs Branch of the Office of Naval Research under contract number N00014-69-A-0141-0008 and project number NR 387-069.

The simulated radar image photo-processing and stereocomparator measurements were performed by personnel of the Mid-Continent Mapping Center, Topographic Division, of the United States Geological Survey in Rolla, Missouri. Their assistance is gratefully acknowledged. Special thanks go to Mr. Gene Lortz who made the stereocomparator measurements and gave measurement advice, and to Mr. Gordon Juneau and Mr. Raymond Hess who gave photographic advice and performed the photo-processing.

REFERENCES

1. D. Levine, *Radargrammetry*, New York: McGraw-Hill, (1960).
2. G. L. LaPrade, "An Analytic Experimental Study of Stereo for Radar", *Photogrammetric Engineering*, 29:294-300, (March 1963).
3. G. E. Carlson, "An Improved Single Flight Technique for Radar Stereo", IEEE Trans. on *Geoscience Electronics*, GE-11, 199-204 (October 1973).
4. G. L. Bair and G. E. Carlson, "Performance Comparison of Techniques for Obtaining Stereo Radar Images", *IEEE Trans.* On Geoscience Electronics, GE-12, (October 1974).
5. G. E. Carlson and G. L. Bair, "Single-Flight Radar Using a Mechanically Slewed Array and an Electrically Squinted Array", Univ. of Mo.-Rolla, *Comm. Sciences Rpt. CSR-73-5*, (November 1973) (AD771434).
6. G. E. Carlson and G. L. Bair, "Comparative Evaluation of an Improved Single Flight Stereo Radar Technique," Univ. of Mo.-Rolla, *Comm. Sciences Rpt CSR-74-1*, (February 1974) (AD774762).
7. M. I. Skolnik, *Radar Handbook*, McGraw-Hill, New York (1970).